Pergamon

Int. J. Heat Mass Transfer. Vol. 40, No. 2, pp. 421–433, 1997

0017–9310/97 $15.00 + 0.00

PII: S0017–9310(96)00112–3

Three-dimensional mixed convection laminar boundary-layer over a horizontal surface in the neighbourhood of a plane of symmetry

A. RIDHA

Université de Caen, Laboratoire de Mécanique, Esplanade de la paix, 14032 Caen Cedex, France and Université P. et M. Curie, Modélisation en Mécanique, CNRS-URA 229 4, place Jussieu, 75252 Paris Cedex 05, France

(*Received* 28 *September* 1995 *and in final form* 31 *January* 1996)

Abstract—The mixed convection laminar boundary-layer flow in the vicinity of the median plane of symmetry of a finite span wedge is considered where one of the wedge surfaces is kept horizontal. The resulting equations thereof depend on the Prandtl number Pr, the buoyancy parameter K and the Falkner–Skan parameter β. The self-similar solutions are found to be non-unique for both aiding and opposing flow regimes where in general two dual solutions are obtained; in certain situations eight solutions prevail. The free convection limit is also treated upon considering the asymptotic equations as $K \to \infty$. Numerical results are presented and discussed for both flows for the prescribed wall temperature and wall heat flux conditions. Copyright © 1996 Elsevier Science Ltd.

1. INTRODUCTION

Three-dimensional (3D) mixed convection boundary-layer flows appear to have received (to the author's knowledge) relatively little attention in the literature in comparison with their 2D counterparts so far; yet in most engineering practices flows are more likely to be rather 3D in nature than not. The difficulty encountered in studying such flows may somewhat be alleviated in considering examples tenable to analyses with a view to providing a deeper insight into the more complex flow situations. In this spirit Yao and Catton [1] considered the laminar boundary-layer over a heated hollow semi-infinite cylinder with its axis aligned parallel to a uniform stream and normal to the direction of gravity. An interesting example of 3D mixed convection is furnished by the work of Eichhorn and Hasan [2] where the buoyancy force acts in a direction perpendicular to that of a free stream flowing past a wedge. The present author [3] in an attempt to study mixed convection in a streamwise corner looked into the simpler case with asymptotic suction when the corner line is kept vertical; this offered the possibility to obtain exact solutions for the Navier–Stokes and energy equations. Recently, the 3D mixed convection boundary-layer flow over a vertical surface near a plane of symmetry was considered [4] and the corresponding similarity equations were found to be non-unique; four solutions were obtained for some situations. In practice it is, of course, more desirable to have non-similar solutions in order to bring out more fully the effect of buoyancy force on forced convection, yet it is nevertheless more convenient to seek first self-similar solutions or approximate perturbation ones based on already existing similarity ones; these solutions would then help to provide approximate correlation formulas for engineering use. Allied to this is the fact that such solutions provide intermediate asymptotics [5] and are therefore of interest by themselves.

In this work we consider 3D mixed convection laminar boundary-layer flow in the neighbourhood of the median plane of symmetry of a wedge of finite span length. In engineering practices, one is more likely to encounter flows past surfaces of finite dimensions and hence the interest in the flow due to this geometry. The external flow velocity vector in the said vicinity assumes under certain circumstances the form $(U, V, W) = U_\infty(x/l)^m\ (1, -my/2x, -mz/2x)$ [4]. The pure forced convection boundary-layer equations corresponding to such an external flow possess dual similar solutions [6, 7] and were, in fact, derived to provide the leading order term in an asymptotic solution corresponding to the boundary conditions for the laminar boundary-layer flow in a streamwise corner [6]. Besides the study of mixed convection in three dimensions arising from the said geometry the evolution of the non-uniqueness in question provides a further motivation for the present work. Here, it is found that the said dual solutions are themselves doubled or quadrupled, in some cases for both aiding and opposing flow conditions. The latter aspect confirms recent results [8] on non-uniqueness in aiding flow situations for some 2D flow examples.

We shall first derive the basic non-similarity equations and then consider the self-similar version thereof. The result is a system of three equations involving a family of three parameters, namely the Falkner–

NOMENCLATURE

A	dummy variable
C	constant
c_f	coefficient of skin friction, $2\tau_w/\rho_\infty U^2$
f, h	dimensionless stream functions, cf. equation (10)
g	gravitational acceleration
Gr	Grashoff number, $\alpha g l^3 \Delta T/\nu^2$
k	thermal conductivity
K	buoyancy parameter, $Gr/Re^{5/2} = \alpha g l^{1/2}\nu^{1/2}\Delta T/U_\infty^{5/2}$
l	characteristic length scale
m	exponent in the power law variation of the flow variables
Nu_x	local Nusselt number, $q_w x/(T_w - T_\infty)$
p	fluid pressure
Pr	Prandtl number, ν/σ
q	heat flux, $-k\,\partial T/\partial y$
r	r co-ordinate in the cylindrical polar co-ordinates system (x, r, ω), cf. Fig. 1
Re	characteristic Reynolds number, $U_\infty l/\nu$
Re_x	local Reynolds number, Ux/ν
T	fluid temperature
ΔT	temperature difference scale
u, v, w	velocity components in the x, y, z-directions
x, y, z	Cartesian co-ordinates: axial, normal and transversal directions
U, V, W	inviscid flow velocity components in the x, y, z-directions
U_∞	characteristic velocity scale.

Greek symbols

α	coefficient of thermal expansion
β	Falkner–Skan parameter, $2m/m+1$
ζ	dummy independent variable
η, ξ	dimensionless independent variables, cf. equation (10)
θ	dimensionless temperature, $(T - T_\infty)/(T_w - T_\infty)$
ω	angular co-ordinate in the cylindrical polar co-ordinates system (x, r, ω), cf. Fig. 1
μ	dynamic viscosity
ν	kinematic viscosity
ρ	fluid density
σ	thermal diffusivity
τ	shear stress
ψ, χ	stream functions, cf. equation (10)
ϕ	velocity potential function.

Subscripts

0, 1, 2, ...	variable in a series expansion
∞	free-stream value of a fluid property
w	wall value.

Superscripts

$\bar{}$	free-convection variable with prescribed T_w
$\hat{}$	free-convection variable with prescribed q_w.

Skan parameter β, Prandtl number Pr, and the buoyancy parameter K. Self-similar solutions of these equations are thereafter presented and discussed for the cases of uniform wall temperature, uniform wall heat flux and the stagnation flow situations. Likewise the corresponding results of the free-convection boundary-layer are also considered; these are obtained on taking the limit $K \to \infty$.

2. ANALYSIS

Consider laminar mixed convection boundary-layer flow over the upper surface of a wedge of a finite span length with the said surface being kept parallel to the horizontal line as shown in Fig. 1. In terms of the Cartesian co-ordinates (x, y, z) the wedge upper surface is given by $y = 0$ and the median plane of symmetry by $z = 0$. In [4] it was shown that the inviscid flow in the vicinity of the median symmetry plane derives from the following potential function

$$\phi = U_\infty \left(\frac{x}{l}\right)^{m+1} \left\{\frac{1}{m+1} - \frac{m}{2}\left(\frac{y}{x}\right)^2 + C\frac{(z^2 - y^2)}{x^2} + O\left(\left(\frac{r}{x}\right)^4\right)\right\}, \quad (1)$$

where U_∞ is a reference velocity scale, m and C are constants with the latter depending on the wedge configuration; this form is valid of course provided that $r/x \ll 1$. For example when $C = 0$ the two-dimensional wedge configuration is retained. Here we shall consider the case $C = -m/4$ which pertains to the situation maximizing the kinetic energy in the said vicinity [4]. It is of interest to recall here that the same form is obtained for streamwise flow along a corner at the outer reaches of the corner boundary-layer side-edge [6]. The corresponding inviscid flow velocity vector associated with the co-ordinates (x, y, z) is $(U, V, W) = U_\infty(x/l)^m(1, -my/2x, -mz/2x)$. This suggests immediately that it is possible to look for a boundary-layer solution in the neighbourhood of the median plane of symmetry in the form

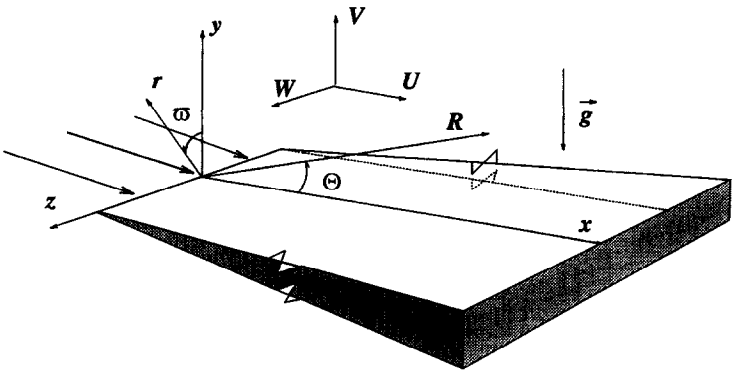

Fig. 1. Flow configuration.

$$u(x,y,z) = u_0(x,y) + z^2 u_2(x,y) + \cdots$$

$$v(x,y,z) = v_0(x,y) + z^2 v_2(x,y) + \cdots$$

$$w(x,y,z) = z w_1(x,y) + z^3 w_3(x,y) + \cdots$$

$$p(x,y,z) = p_0(x,y) + \tfrac{1}{2} z^2 p_2(x,y) + \cdots$$

$$T(x,y,z) = T_0(x,y) + z^2 T_2(x,y) + \cdots. \quad (2)$$

From the outset we assume constant fluid properties and hence it follows that upon applying the boundary-layer and Boussinesq approximations we find to the leading order in z the following governing equations

$$\frac{\partial u}{\partial x} + \frac{\partial v}{\partial y} + w = 0, \quad (3)$$

$$u\frac{\partial u}{\partial x} + v\frac{\partial u}{\partial y} = -\frac{1}{\rho_\infty}\frac{\partial p_0}{\partial x} + \nu\frac{\partial^2 u}{\partial y^2} \quad (4)$$

$$\frac{\partial p_0}{\partial y} = \alpha \rho_\infty g (T - T_\infty) \quad (5)$$

$$u\frac{\partial w}{\partial x} + v\frac{\partial w}{\partial y} + w^2 = -\frac{p_2}{\rho_\infty} + \nu\frac{\partial^2 w}{\partial y^2} \quad (6)$$

$$u\frac{\partial T}{\partial x} + v\frac{\partial T}{\partial y} = \frac{\nu}{Pr}\frac{\partial^2 T}{\partial y^2} \quad (7)$$

where for brevity all subscripts save for those of the pressure have been dropped out. The pressure term p_0 accounts, in conformity with the boundary-layer approximations, for the hydrostatic pressure contribution the gradient of which is given in equation (5). The pressure gradient in the z-direction is retained through p_2 which, according to the boundary-layer approximation, can be shown to be independent of y; its value is obtained of course from the free stream conditions and it comes out that $p_2 = 0.25m(m-2)\rho_\infty U_\infty^2 x^{2m-2}$. Further, it is usually convenient to integrate equation (5) with respect to y in order to express p_0 in terms of T in equation (4) which yields

$$u\frac{\partial u}{\partial x} + v\frac{\partial u}{\partial y} = g\alpha\frac{\partial}{\partial x}\int_y^\infty (T - T_\infty)\,dy + \nu\frac{\partial^2 u}{\partial y^2}. \quad (8)$$

In this work two different cases will be considered; (i) prescribed wall temperature, $T_w = T_\infty + \Delta T(x/l)^{(5m-1)/2}$; (ii) prescribed wall heat flux, $q_w = k\Delta T\,[(1+m)U_\infty/2l\nu]^{1/2}(x/l)^{3m-1}$. In conformity with the definition of T_w a positive or negative sign of ΔT will designate therefore a heated or a cooled surface.

The equations to be solved henceforth are (3), (6), (7) together with (8) subject to the following boundary conditions

$$u = v = w = 0, \quad \text{with either for case (i)}$$

$$T = T_w \quad \text{at} \quad y = 0$$

$$\text{or for case(ii)} \quad -k\frac{\partial T}{\partial y} = q_w$$

$$u \to U_\infty (x/l)^m \quad w \to -\frac{m}{2}(x/l)^{m-1}$$

$$T \to T_\infty \quad \text{as} \quad y \to \infty. \quad (9)$$

Next, the governing equations are rendered dimensionless on introducing the stream functions ψ and χ in addition to the following transformation variables

$$u = \frac{\partial \psi}{\partial y} \quad v = -\left(\frac{\partial \psi}{\partial x} + \chi\right) \quad w = \frac{\partial \chi}{\partial y} \quad \beta = \frac{2m}{1+m}$$

$$\psi = \left[\frac{2l\nu U_\infty}{1+m}\right]^{1/2}\left(\frac{x}{l}\right)^{(m+1)/2} f(\xi,\eta)$$

$$\chi = \left[\frac{2\nu U_\infty/l}{1+m}\right]^{1/2}\left(\frac{x}{l}\right)^{(m-1)/2} h(\xi,\eta)$$

$$T - T_\infty = \Delta T\left(\frac{x}{l}\right)^{(5m-1)/2}\theta(\xi,\eta)$$

$$\xi = \frac{x}{l} \quad \eta = \left[\frac{1+m}{2l\nu}U_\infty\right]^{1/2}\left(\frac{x}{l}\right)^{(m-1)/2} y. \quad (10)$$

The transformation yields

$$f''' + [(2-\beta)h + f]f'' + \beta(1 - f'^2) + K(2-\beta)^{1/2}\left[2\beta\int_\eta^\infty \theta(\xi,\zeta)\,d\zeta + (1-\beta)\eta\theta\right]$$

$$= \xi(2-\beta)\left[f'f'_\xi - f''f_\xi - K(2-\beta)^{1/2}\int_\eta^\infty \theta(\xi,\zeta)_\xi \,\mathrm{d}\zeta\right] \tag{11}$$

$$h''' + [(2-\beta)h+f]h'' + [2(1-\beta)f' - (2-\beta)h']h' - \frac{\beta(3\beta-4)}{4(2-\beta)} = \xi(2-\beta)(f'h'_\xi - h''f_\xi) \tag{12}$$

$$\frac{1}{Pr}\theta'' + [(2-\beta)h+f]\theta' + (1-3\beta)f'\theta = \xi(2-\beta)(f'\theta_\xi - \theta' f_\xi) \tag{13}$$

where $(\cdot)' = \partial(\cdot)/\partial\eta$ and $(\cdot)_\xi = \partial(\cdot)/\partial\xi$. The corresponding boundary conditions, equations (9) become

$$\eta = 0 \quad f = h = f' = h' = 0$$

$$\text{with either for case (i)} \quad \theta = 1$$

$$\text{or for case(ii)} \quad \theta' = -1,$$

$$\eta \to \infty; \quad f' \to 1, \quad h' \to -\frac{\beta}{2(2-\beta)}, \quad \theta \to 0. \tag{14}$$

Here instead of seeking the non-similar solutions of equations (11)–(13) attention will be confined to the solutions of the similarity equations obtained thereof on setting $(\cdot)_\xi = 0$. The result is the following set of ordinary differential equations

$$f''' + [(2-\beta)h+f]f'' + \beta(1-f'^2) + K(2-\beta)^{1/2}\left[2\beta\int_\eta^\infty \theta(\zeta)\,\mathrm{d}\zeta + (1-\beta)\eta\theta\right] = 0 \tag{15}$$

$$h''' + [(2-\beta)h+f]h'' + [2(1-\beta)f' - (2-\beta)h']h' = \frac{\beta(3\beta-4)}{4(2-\beta)} \tag{16}$$

$$\frac{1}{Pr}\theta'' + [(2-\beta)h+f]\theta' + (1-3\beta)f'\theta = 0 \tag{17}$$

subject to the boundary condition given by equations (14). In equations (15)–(17) a prime denotes differentiation with respect to η.

At this juncture it is worthwhile to note that when $K = 0$ identically equations (15) and (16) as well as the corresponding boundary conditions reduce to the boundary conditions of the corner boundary-layer side-edge [6] which were found to have dual solutions in the range $-0.03678 \leqslant \beta \leqslant 1.211$ [7]. Results that will be presented later show that the said solutions are doubled or quadrupled when $|K| \to 0$ for some situations; this occurs for both aiding and opposing flow conditions.

The free-convection situation corresponding to the flow configuration treated above is obtained on considering the limit $K \to \infty$ and is presented in the following section.

3. THE FREE-CONVECTION LIMIT, $K \to \infty$

As K becomes sufficiently greater than unity the flow approaches the free-convection limit. Two distinct cases are obtained depending upon the wall thermal condition whether it is defined by a prescribed wall temperature or wall heat flux. An outline of the derivation of these respective limits is given below.

3.1. *Prescribed wall temperature condition, case* (i)

Here we set

$$f = K^{1/5}\bar{f}, \quad h = K^{1/5}\bar{h}, \quad \theta = \bar{\theta}, \quad \eta = K^{1/5}\bar{\eta} \tag{18}$$

which when substituted in equations (15)–(17) yields

$$\bar{f}''' + [(2-\beta)\bar{h}+\bar{f}]\bar{f}'' + \beta K^{-4/5} - \beta\bar{f}'^2 + (2-\beta)^{1/2}\left[2\beta\int_{\bar{\eta}}^\infty \bar{\theta}(\zeta)\,\mathrm{d}\zeta + (1-\beta)\bar{\eta}\bar{\theta}\right] = 0 \tag{19}$$

$$\bar{h}''' + [(2-\beta)\bar{h}+\bar{f}]\bar{h}'' + [2(1-\beta)\bar{f}' - (2-\beta)\bar{h}']\bar{h}' = \frac{\beta(3\beta-4)}{4(2-\beta)}K^{-4/5} \tag{20}$$

$$\frac{1}{Pr}\bar{\theta}'' + [(2-\beta)\bar{h}+\bar{f}]\bar{\theta}' + (1-3\beta)\bar{f}'\bar{\theta} = 0 \tag{21}$$

subject to the boundary conditions

$$\bar{\eta} = 0; \quad \bar{f} = \bar{h} = \bar{f}' = \bar{h}' = 0, \quad \bar{\theta} = 1$$

$$\bar{\eta} \to \infty; \quad \bar{f}' \to K^{-2/5},$$

$$\bar{h}' \to -\frac{\beta}{2(2-\beta)}K^{-2/5}, \quad \bar{\theta} \to 0. \tag{22}$$

Here, a prime designates differentiation with respect to $\bar{\eta}$. These equations suggest looking for expansions of the form

$$\bar{A} = \bar{A}_0 + K^{-2/5}\bar{A}_1 + K^{-4/5}\bar{A}_2 \ldots, \tag{23}$$

where A stands for f, h or θ. Substituting these expansions in equations (19)–(21) gives to the zeroth order in K the following system of equations

$$\bar{f}'''_0 + [(2-\beta)\bar{h}_0 + \bar{f}_0]\bar{f}''_0 - \beta\bar{f}'^2_0 + (2-\beta)^{1/2}\left[2\beta\int_{\bar{\eta}}^\infty \bar{\theta}_0(\zeta)\,\mathrm{d}\zeta + (1-\beta)\bar{\eta}\bar{\theta}_0\right] = 0 \tag{24}$$

$$\bar{h}'''_0 + [(2-\beta)\bar{h}_0 + \bar{f}_0]\bar{h}''_0 + [2(1-\beta)\bar{f}'_0 - (2-\beta)\bar{h}'_0]\bar{h}'_0 = 0 \tag{25}$$

$$\frac{1}{Pr}\bar{\theta}''_0 + [(2-\beta)\bar{h}_0 + \bar{f}_0]\bar{\theta}'_0 + (1-3\beta)\bar{f}'_0\bar{\theta}_0 = 0 \tag{26}$$

together with the following boundary conditions

$$\left.\begin{aligned} \bar{f}_0(0) = \bar{h}_0(0) = \bar{f}'_0(0) = \bar{h}'_0(0) = 0 \quad & \bar{\theta}_0(0) = 1 \\ \bar{f}'_0(\infty) = \bar{h}'_0(\infty) = 0 \quad & \bar{\theta}_0(\infty) = 0 \end{aligned}\right\}. \tag{27}$$

Numerical solutions of these equations are presented and discussed in Section 4.

3.2. *Prescribed wall heat flux condition, case* (ii)

For this case we write

$$f = K^{1/6}\hat{f} \quad h = K^{1/6}\hat{h} \quad \theta = K^{-1/6}\hat{\theta} \quad \eta = K^{-1/6}\hat{\eta} \tag{28}$$

which upon substitution in equations (15)–(17) leads to

$$\hat{f}''' + [(2-\beta)\hat{h} + \hat{f}]\hat{f}'' + \beta K^{-2/3} - \beta\hat{f}'^2 + (2-\beta)^{1/2}\left[2\beta\int_{\hat{\eta}}^{\infty}\hat{\theta}(\zeta)\,d\zeta + (1-\beta)\hat{\eta}\hat{\theta}\right] = 0 \tag{29}$$

$$\hat{h}''' + [(2-\beta)\hat{h} + \hat{f}]\hat{h}'' + [2(1-\beta)\hat{f}' - (2-\beta)\hat{h}']\hat{h}' = \frac{\beta(3\beta-4)}{4(2-\beta)}K^{-2/3} \tag{30}$$

$$\frac{1}{Pr}\hat{\theta}'' + [(2-\beta)\hat{h} + \hat{f}]\hat{\theta}' + (1-3\beta)\hat{f}'\hat{\theta} = 0 \tag{31}$$

supplemented by the boundary conditions

$$\hat{\eta} = 0 \quad \hat{f} = \hat{h} = \hat{f}' = \hat{h}' = 0 \quad \theta = 1$$

$$\hat{\eta} \to \infty \quad \hat{f}' \to K^{-1/3}$$

$$\hat{h}' \to -\frac{\beta}{2(2-\beta)}K^{-1/3} \quad \theta \to 0 \tag{32}$$

where a prime in this case denotes differentiation with respect of $\hat{\eta}$. Again, these equations suggest expansions of the form

$$\hat{A} = \hat{A}_0 + K^{-1/3}\hat{A}_1 + K^{-2/3}\hat{A}_2 \ldots, \tag{33}$$

where in this case A represents f, h or θ. Likewise we seek the zeroth order equations in K which come out to be exactly of the same form as equations (24)–(26) subject to similar boundary conditions as in equations (27) save for $\bar{\theta}_0(0) = 1$ being replaced by $\hat{\theta}_0'(0) = -1$. Numerical results pertaining to this case are presented and discussed in the following section.

4. RESULTS AND DISCUSSIONS

As mentioned earlier the pure convection version (i.e. with $K = 0$ identically) of equations (15), (16) subject to the boundary conditions given in equations (14) have dual solutions in function of β [6, 7]; for a given value of β the solution having the higher $f''(0)$ value will be referred to herein as the upper branch (U) solution and that having the lower value as the lower branch (L) solution. In the mixed convection version [equations (15)–(17)], these dual solutions are doubled or quadrupled in the admissible space of (β, K). For want of a precise terminology, it is convenient for a given β (U) solution to denote the upper branch solution obtained on varying K by (UU) and likewise the lower branch solution by (UL) with the first letter referring to the β upper branch solution. An upper or lower solution in this case depends on having a higher or lower value of $f''(0)$. Similarly (LU) or (LL) will refer to the upper or lower branch solutions stemming out of the (L) pure convection solution. On the other hand, where the dual solutions are quadrupled, they are found to have no physical sense (save for the corresponding upper branch solutions (UU) and (LU)) either because $\theta'(0) > 0$ or $\theta < 0$ for some range of η. Nevertheless this should not belittle these results since it is quite plausible that analogue equations could arise from some other real situations where the solutions could have a physical sense; this is of course in addition to the mathematical interest that such equations may provide.

Next, apart from the non-uniqueness of the solutions, the mere presence of the three parameters (Pr, K, β) in the formulation gives rise to a considerable amount of results to present and analyse. For brevity as well as for practical considerations we have opted therefore to consider only the uniform wall temperature $\beta = 1/3$, uniform wall heat flux $\beta = 0.5$ and stagnation flow $\beta = 1$ situations with $Pr = 1$ throughout. With regards to the natural convection case only results pertaining to $Pr = 1$ are presented and discussed. All numerical results are obtained by using a fourth-order Runge–Kutta method programmed in double precision following the parallel shooting algorithm [9]; convergence to a solution is considered satisfactory when all the outer boundary conditions are satisfied within a tolerance equal to or less than 10^{-8}.

Besides the velocity and temperature fields, the primary quantities of interest are, in general, the local Nusselt number $Nu_x = q_w x/(T_w - T_\infty)$ and the local wall shear stress $\tau_w = \mu(\partial u/\partial y)_{y=0}$ expressed for convenience in terms of the skin friction coefficient, $c_f = 2\tau_w/\rho_\infty U^2$. It comes out that we have for the mixed convection regime

$$(2-\beta)^{1/2}c_f Re_x^{1/2}/2 = f''(0);$$

$$-(2-\beta)^{1/2}Nu_x Re_x^{-1/2} = \theta'(0) \quad \text{if } T_w \text{ is prescribed, case (i);}$$

$$(2-\beta)^{1/2}Nu_x Re_x^{-1/2} = 1/\theta(0) \quad \text{if } q_w \text{ is prescribed, case(ii)} \tag{34}$$

and for the free-convection

$$-(2-\beta)^{1/2}Nu_x Re_x^{-1/2}K^{-1/5} = \bar{\theta}'(0) \quad \text{for case (i);}$$

$$(2-\beta)^{1/2}Nu_x Re_x^{-1/2}K^{-1/6} = 1/\hat{\theta}(0) \quad \text{for casc(ii).} \tag{35}$$

Consequently, it suffices therefore to present the corresponding results in terms of $f''(0)$, $h''(0)$ with either $\theta'(0)$ or $\theta(0)$.

Results for the quantities defined in equations (34) are shown in Fig. 2(a) where for the purpose of comparison we have added the corresponding 2D results

(a)

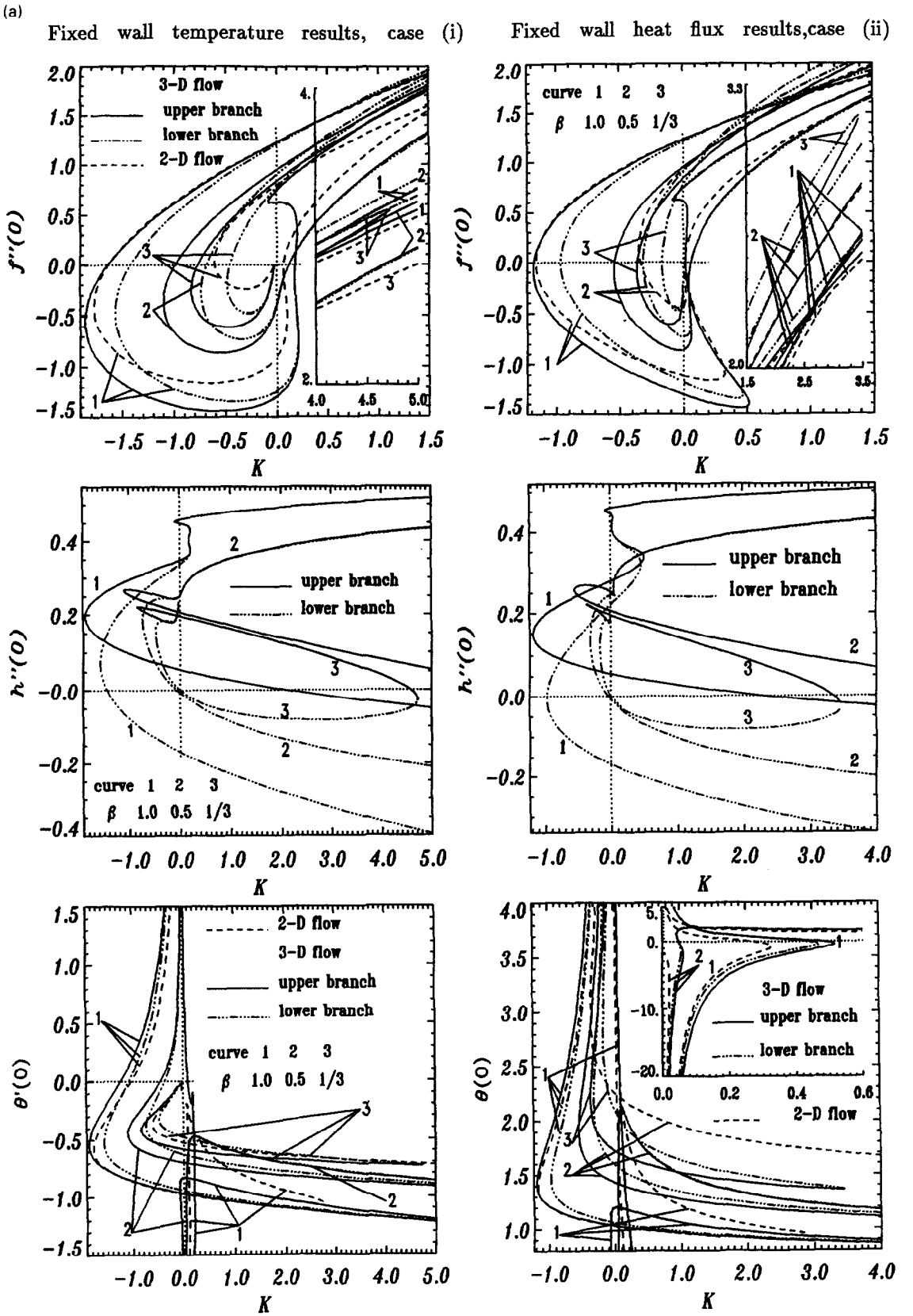

Fig. 2. (a) Graphs of $f''(0)$, $h''(0)$ as well as of $\theta'(0)$ or $\theta(0)$ for case (i) or (ii), respectively. (b) Graphs of $f''(0)$, $h''(0)$ as well as of $\theta'(0)$ or $\theta(0)$ for case (i) or (ii), respectively; solutions that could have a physical sense.

(b)

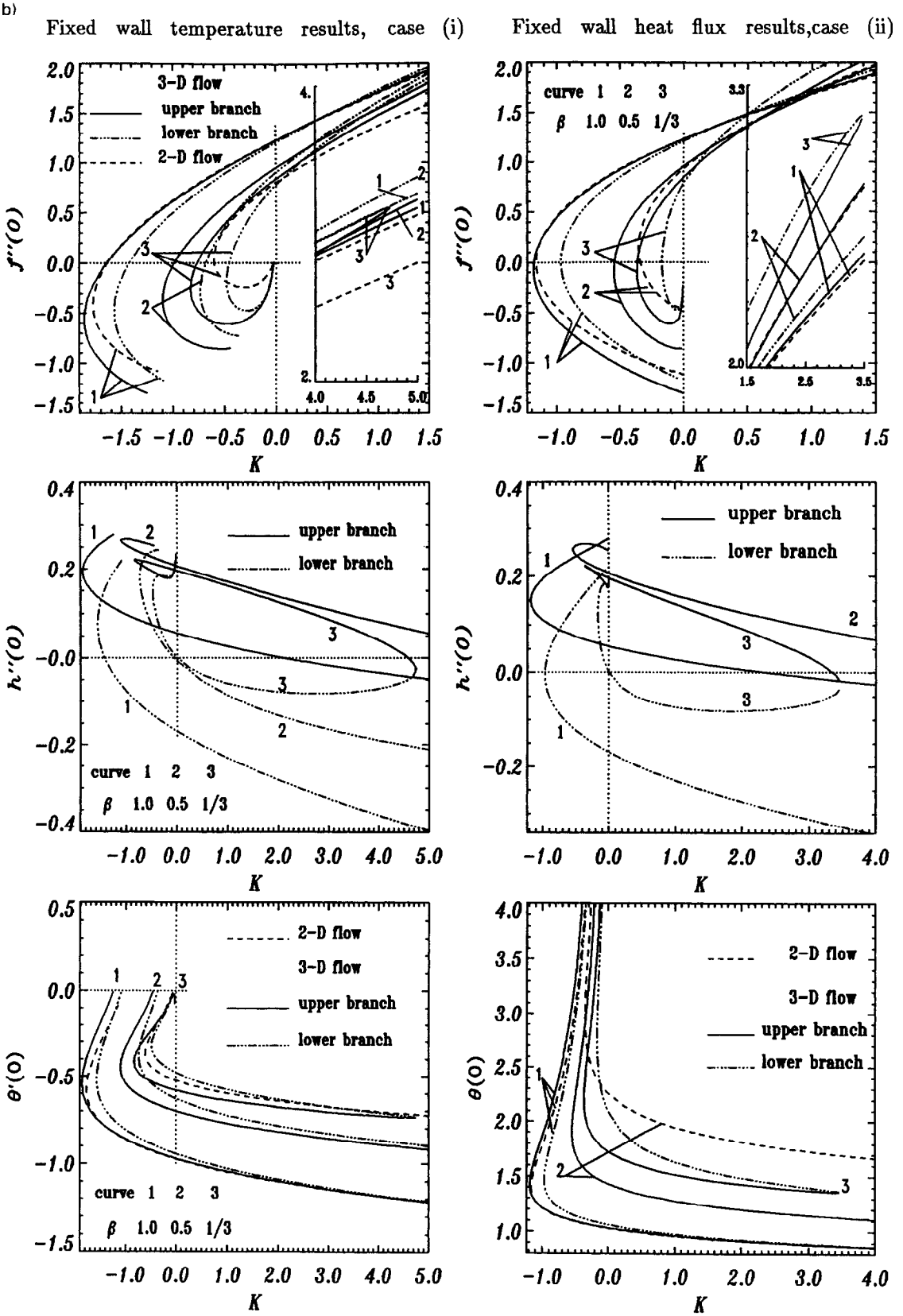

Fig. 2—*Continued.*

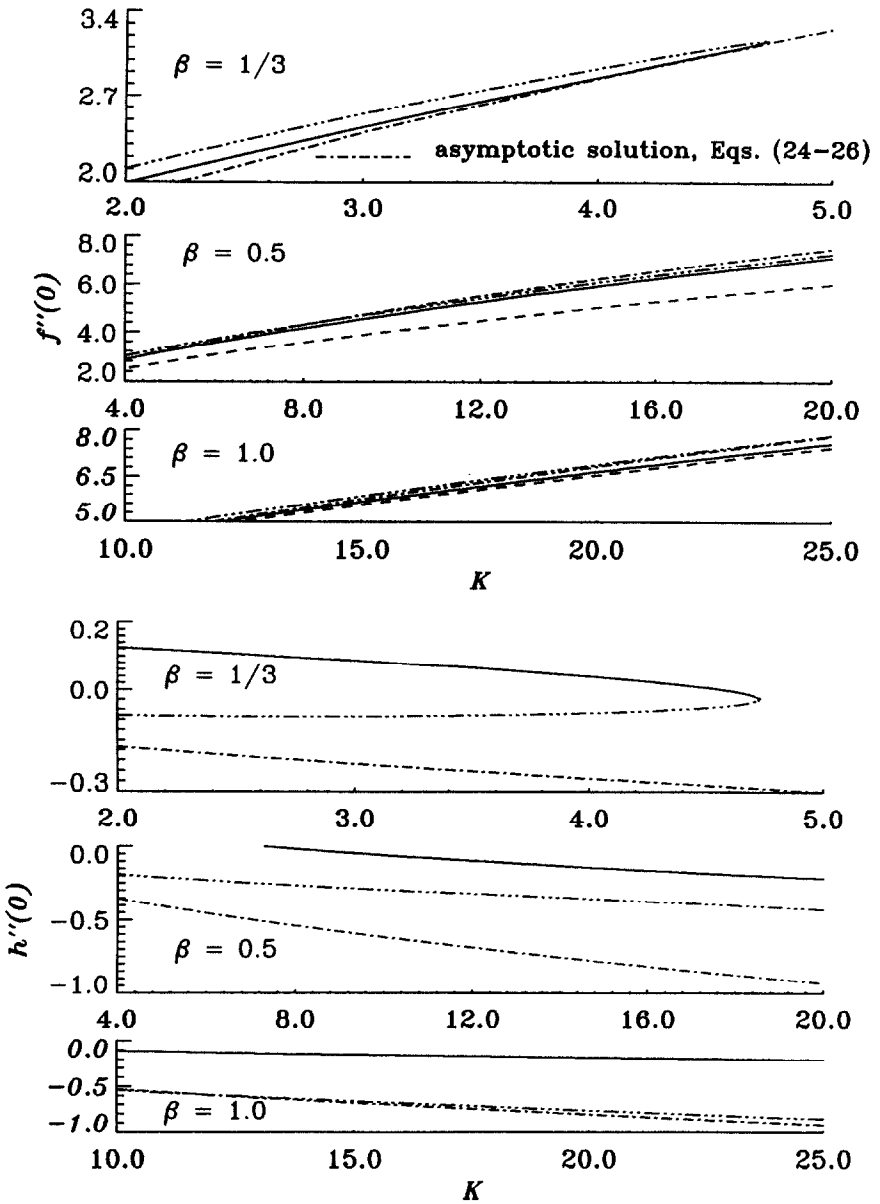

Fig. 3. Comparison of the skin friction results obtained from equations (15)–(17) and (24)–(26). The broken line, - - -, designates the 2D corresponding results [8].

over a horizontal surface, [8]. A number of interesting observations can be made here. First, without any doubt the most striking feature resides in the non-uniqueness of these results for opposing as well as aiding flow conditions. Until quite recently [4, 8, 10] non-uniqueness of laminar mixed convection boundary-layer solutions were only reported for opposing flow ($K < 0$) conditions and were, in general, confined to dual solutions. In the present problem eight solutions are obtained for certain (β, K) ranges; this is twice the number obtained for the corresponding problem over a vertical surface [4]. In both, only two aiding flow solutions have physical sense for reasons that have already been outlined above; these happen to be always the (UU) and (LU) solutions. The remaining corresponding four opposing flow solutions, on the other hand, have all physical sense. For clarity, we have reproduced only the latter solutions on Fig. 2(b).

Keeping in mind that self-similar solutions represent asymptotic situations [5] it is plausible then to argue that the flow they represent could take place depending on how its conditions may be approached. In this respect we may for instance be reminded as remarked in [11] that Spangenberg *et al.* [12] have reported in their experimental work on turbulent boundary layer under strong adverse pressure gradient that dual solutions were obtained in function of how the pressure gradient was realized. Another example of non-unique flows is reported by Aidun *et al.* [13] where they have observed experimentally that the primary steady state flow in a through-flow lid-

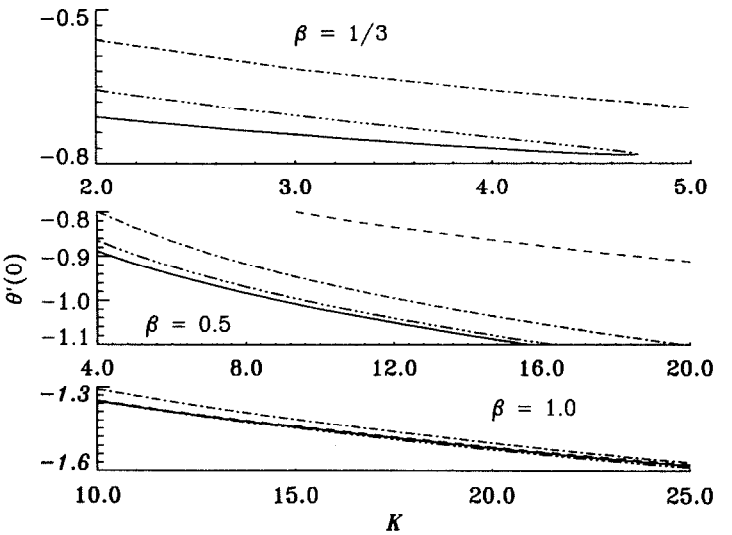

Fig. 4. Comparison between wall heat transfer results due to equations (15)–(17) and (24)–(26). The broken line, - - -, designates the 2D corresponding results [8].

driven cavity was non-unique and "only one of the multiple steady-state patterns can stabilize in the cavity." As regards the present results, such a situation is of course only possible should the said flow corresponding to one of the aforementioned non-unique solutions (if it exists at all in practice) be stable enough to be "reproduced" experimentally. It is pertinent to recall here that such paradoxes are often encountered in viscous flows (see [14]) and may perhaps be resolved by a stability analysis of the kind used for example in [7, 15, 16] which is beyond the scope of the present work.

Second, the velocity field results are observed to be regular and continuous across $K = 0$ whereas those due to the temperature field are discontinuous thereat; this intriguing behaviour is shown in [8] to spring out from the fact that the buoyancy parameter K arises in a linear multiple of the temperature function θ in the streamwise momentum equation. The said regularity is only possible should $K\theta$ remain finite and regular at this vicinity; indeed this is born out to be the case in situations examined in [4, 8, 10] as well as in the present one.

Third, amongst the results considered in this work those of the uniform wall temperature case $\beta = 1/3$ seem to be the most interesting. Here, both the (UU) and (LU) end in a turning point singularity at $K \simeq 4.732$ where their respective $f''(0)$, $h''(0)$, $\theta'(0)$ solutions join with each other. Thus three critical points arise for this case; two for the opposing flow regime; one for each of the (U) and (L) branch solutions, in addition to the turning point in question. Note that by critical point it is meant that point below or above the value of K thereat no solution exists. A similar tendency is also observed as $K \to -0$. Close examination of the results reveals that the velocity and temperature fields solutions converge to the same solution for both branches at the aiding flow critical point (see Fig. 6) while they remain distinct as $K \to -0$ (see Fig. 5). For $\beta = 1$ or 0.5, computations were continued up to $K = 50$ with the former trend being not repeated. A deeper insight into this trend requires certainly a detailed asymptotic analysis in the neighbourhood of $\beta = 1/3$ which is beyond the scope of the present work. Nevertheless, comparison with the results obtained from the asymptotic equations (24)–(26) which are shown in Figs. 3 and 4 may be helpful at this juncture. Here, it is observed that the main flow non-dimensional skin friction results expressed in terms of $f''(0)$ practically merge with those computed via the said equations for $K > 4.0$. The corresponding results pertaining to the secondary cross-flow display, on the other hand, appreciable quantitative differences. Perhaps the following order term in the asymptotic solution is required to draw a satisfactory conclusion in this respect. As regards the wall heat transfer results there is a difference in the respective solutions of order 21%. For $\beta = 1$ or 0.5 situations the comparison is fairly good as is evident from Figs. 3 and 4. Note that for the prescribed wall heat flux case a similar behaviour obtains when $\beta = 1/3$.

Fourth, a further remark worthy of making is that the (LL) solutions give rise to $f''(0)$, $h''(0)$, $\theta'(0)$ [or $\theta'(0)$ in case (ii)] results that are practically the same as those due to the (UL) for $K > 0$. However, the corresponding flow and temperature fields remain nevertheless quite different; it should be recalled here that these solutions bear no physical sense as explained before.

In so far as comparisons with the 2D flow results are concerned it is observed that 3D ones for $f''(0)$, $\theta'(0)$ or $\theta(0)$ appear to have no definite pattern throughout. For instance, for the stagnation flow condition $\beta = 1$ the 2D results lie between those of (UU) and (LU) solutions and almost coincide with them for

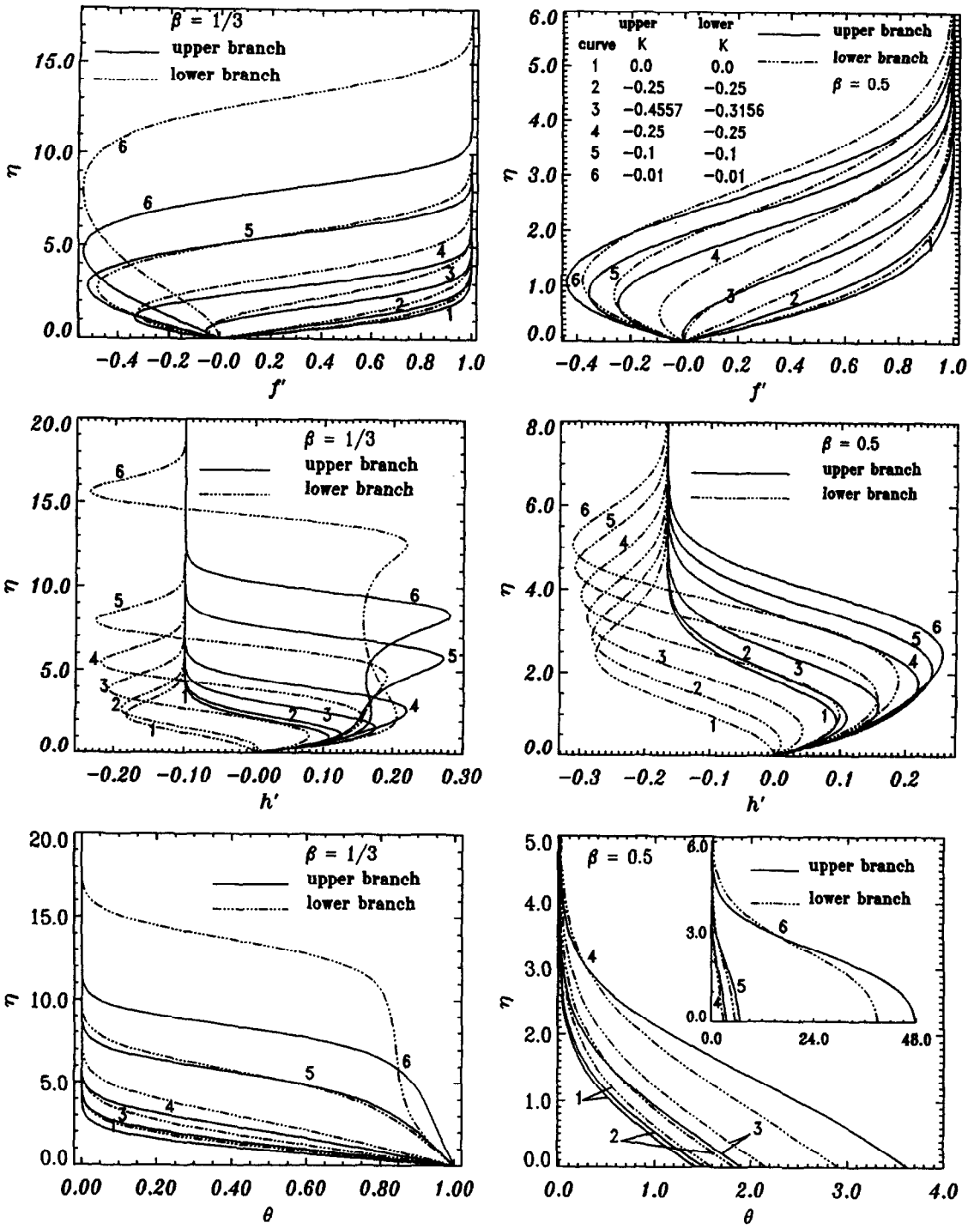

Fig. 5. Uniform wall temperature $\beta = 1/3$ and uniform wall heat flux $\beta = 0.5$ results. For the former case, graphs of f', h', θ are, as per order of numbering, for $K = 0.0, -0.5, -0.83162, -0.5, -0.1, -0.05$ due to the upper branch solutions and for $K = 0.0, -0.25, -0.4848, -0.3, -0.1, -0.027$ due to the lower branch solutions. Graphs number 3 denote results at the critical point.

$K > 0$. Meanwhile, under opposing flow conditions this tendency is lost as the critical point is approached with the (LU) solutions having the greater departure therefrom. On the other hand when $\beta = 0.5$ or $\beta = 1/3$ for both case (i) and (ii) it is seen that the 2D results lie between those of the (UU) and (LU) only in the close vicinity of $K = 0$.

All numerical results presented herein are computed, whenever possible, up to $K = 50$. For $\beta = 0.5$ all solutions terminates in a singularity as $K \rightarrow$

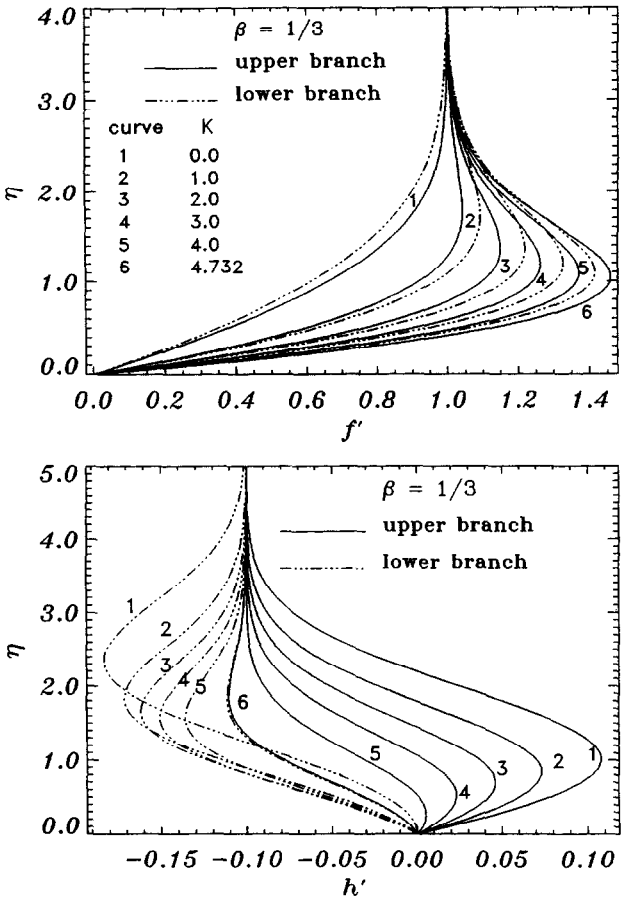

Fig. 6. Uniform wall temperature $\beta = 1/3$ results: evolution of the aiding flow velocity profiles f' and h' in function of K; note that profiles number 6 due to upper and lower branches coincide with each other.

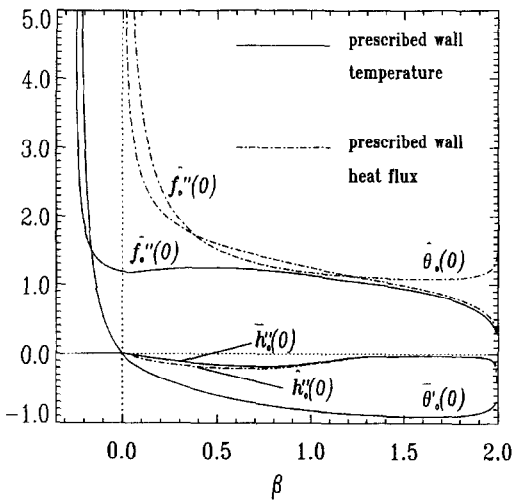

Fig. 7. Free-convection results. Graphs of $\bar{f}''_0(0)$, $\bar{h}''_0(0)$, $\bar{\theta}'_0(0)$ [respectively $\hat{f}''_0(0)$, $\hat{h}''_0(0)$, $\hat{\theta}'_0(0)$] for the prescribed wall temperature (respectively prescribed wall heat flux) distribution.

-0 and consequently solutions were computed up to $K = 50$ for the (UU) and (LU) solutions only.

The velocity and temperature fields results for the uniform wall temperature or heat flux conditions are illustrated in Figs. 5 and 6. Again those pertaining to the former conditions are worthy of some comments first. Separation profiles are obtained in the vicinity of $K \simeq -0.77$ for the (UU) solution and near $K \simeq -0.46$ for the (LU) solution ahead of the critical point in both; this point occurs at $K = -0.83162$ for the former and at $K = -0.4848$ for the latter solutions. In the separation zone the temperature gradient becomes smaller and consequently a thicker thermal boundary layer is obtained. Yet, it is doubtful whether in practice one could obtain flows under these conditions of separation since the mere presence of a zero wall shear stress render the flow unstable to small perturbations.

Next, it is seen that the secondary cross-flow velocity (as represented by h') undergoes a peculiar behaviour which resembles very closely that obtained in the corresponding problem on a vertical surface [4] although it is somewhat less pronounced herein; there, the wall uniform temperature conditions occurs at $\beta = 2/3$. It is felt therefore that further discussion or presentation of the evolution of cross-flow velocity vector in the $(y\text{–}z)$ plane are not needed here with regards to the opposing flow regime. Both are qualitatively the same when due differences are taken into account. Perhaps one needs only point out the double velocity reversal taking place in the h' profile in (LL) solutions for both situations.

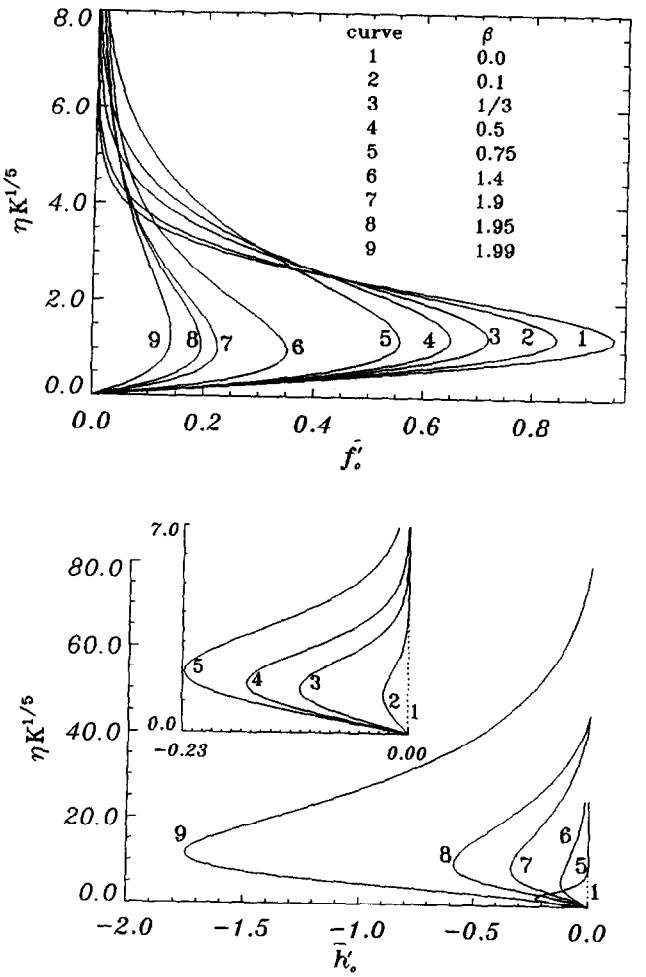

Fig. 8. Free-convection results. Velocity $\bar{f}'_0$, $\bar{h}'_0$ profiles for the prescribed wall temperature distribution.

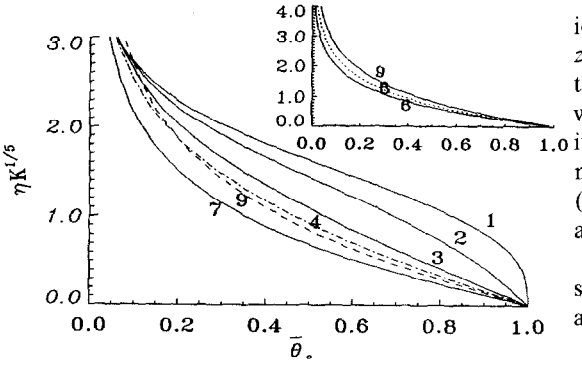

Fig. 9. Free-convection results. Temperature $\bar{\theta}_0$ profiles for the prescribed wall temperature distribution.

In Fig. 6 graphs of the dual solutions arising under aiding flow conditions are depicted. The evolution of main stream velocity in function of K shows that the (U) solutions profiles approach the free stream conditions faster than those due to their (L) solutions counterparts whereas the overshooting of the said conditions is greater in the latter results. This behaviour is coupled in the latter case to an inflow in the y–z plane towards the median plane of symmetry. For the former the flow in the immediate vicinity of the wall is driven away from the said plane but towards it in the upper half of the boundary layer. The thickness of the latter is therefore seen to be greater in the (L) solutions than those pertaining to the (U) ones and likewise for the thermal boundary layer.

Results with uniform wall heat flux condition are self-explaining and, in relative terms, warrant no additional comments herein.

Let us consider next the free-convection results for the skin friction and wall heat transfer which are depicted in Fig. 7. For the prescribed wall heat flux condition $\hat{f}''_0(0)$ approaches ∞ as $\beta \to 0$ while it approaches zero as $\beta \to 2$ with the solution terminating in a singularity at both ends. A linear relationship between these quantities appears to prevail for intermediate values of β between 0.5 and 1.5. A similar trend is observed to be followed by the wall temperature near the lower end of β; here $\hat{\theta}_0(0) \to \infty$ which implies that $Nu_x \to 0$ according to equation (35). As β increases $\hat{\theta}_0(0)$ decreases and (and hence

Nu_x increases) tends to remain almost constant before rising up rapidly (Nu_x getting smaller again) near $\beta = 2$. Allied to this the secondary cross-flow skin friction is small and negative throughout. Examination of the prescribed wall temperature results reveals an analogue behaviour for $\bar{f}''_0(0)$ apart from two differences. First, the solution terminates in a singularity near $\beta = -0.25$ instead of $\beta = 0$ with zero wall heat transfer occurring at the latter point. Second, solutions with $\beta < 0$ have in consequence no physical sense for the same reasons as explained in similar situations for mixed convection.

In Fig. 8 are depicted the velocity profiles $\bar{f}'_0$ and $\bar{h}'_0$ in function of β and the corresponding temperature profiles are shown in Fig. 9. The maximum value of the streamwise velocity is observed to occur at $\beta = 0$ and decreasing uniformly towards a minimum at the upper β end. Note that at the former end we have a 2D flow situation. On the other hand, the secondary cross-flow velocity is seen to grow larger to a maximum absolute value as $\beta \to 2$; this is coupled to an algebraic decay behaviour towards the ambient conditions as this β limit is approached. Tied to this a somewhat greater momentum boundary layer thickness obtains than its thermal counterpart. A similar trend is also observed with regards to the prescribed wall heat flux results. Again the cross flow-velocity vector evolution in the $(y$–$z)$ plane in function of β displays qualitatively similar trends as in the corresponding situation over a vertical surface [4] and are therefore not presented herein. Apart from these observations there seems to be no need to make any further comment.

REFERENCES

1. L. S. Yao and I. Catton, Buoyancy cross-flow effects on longitudinal boundary layer flow along a heated horizontal hollow cylinder, *ASME J. H. Transfer* **99,** 122–124 (1977).
2. R. Eichhorn and M. M. Hasan, Mixed convection about a vertical surface in cross-flow: a similarity solution, *ASME J. Heat Transfer* **102,** 775–777 (1980).
3. A. Ridha, Laminar mixed convection in a corner with suction, *Mech. Res. Commun.* **17**(5), 327–335 (1990).
4. A. Ridha, Three-dimensional mixed convection laminar boundary-layer near a plane of symmetry, *Int. J. Engng Sci.* **34** (6), 659–675 (1966).
5. G. I. Barenblatt and Ya. B. Zel'dovich, Self-similar solutions as intermediate asymptotics, *Adv. Fluid Mech.* **12,** 285–312 (1972).
6. A. Ridha, Sur la couche limite incompressible laminaire le long d'un dièdre, *C. R. Acad. Sci. Paris* **311** (série II), 1123–1128 (1990).
7. A. Ridha, On the dual solutions associated with boundary-layer equations in a corner, *J. Engng Math.* **26,** 525–537 (1992).
8. A. Ridha, Aiding flows non-unique similarity solutions of mixed-convection boundary layer equations, *Z. Angew, Math. Phys.* **46**(3), 341–352 (1996).
9. Herbert B. Keller, *Numerical Methods For Two-Point Boundary-Value Problems.* Dover, New York (1992).
10. A. Ridha, Convection mixte tridimensionnelle sur une plaque plane horizontale au voisinage d'un plan de symétrie. In *Actes du 12e Congrès Français de Méanique Strasbourg* 1995, Vol. 2, pp. 281–284. Association Universitaire de Mécanique.
11. N. Afzal and T. Hussain, Mixed convection over a horizontal plate, *ASME J. Heat Transfer* **106,** 240–241 (1984).
12. W. G. Spangenberg, W. R. Rowland and N. E. Mease. In *Fluid Mechanics of Internal Flows* (edited by G. Sovran), pp. 110–150. Elsevier, Amsterdam (1967).
13. C. K. Aidun, N. G. Triantafillopoulos and J. D. Benson, Global stability of a lid-driven cavity with throughflow, *Physics Fluids A* **3,** 2081–2091 (1991).
14. M. A. Goldshtik, Viscous-flow paradoxes, *Annu. Rev. Fluid Mech.* **22,** 441–472 (1990).
15. J. M. Merkin, On dual solutions occurring in mixed-convection in porous medium, *J. Engng Math.* **20,** 171–179 (1985).
16. H. Steinrück, Mixed convection over a horizontal plate: self-similar and connecting boundary-layer flows, *Fluid Dyn. Res.* **15,** 113–127 (1995).

Résumé—On considère la couche-limite laminaire en convection mixte au voisinage d'un plan de symétrie sur la surface horizontale d'un dièdre d'une envergure finie. Ce problème fournit des équations différentielles qui dépendent du nombre de Prandtl Pr, du paramètre de flottement K et celui de Falkner–Skan β. On montre (par voie numérique) que les équations autosemblables ont des solutions non-uniques pour une surface refroidie ou chauffée. Ces équations peuvent avoir, en général, quatre solutions mais dans certains cas elles en possédent huit. En plus, on traite le cas limite ($K \to \infty$) de la convection libre. Des résultas numériques, se rapportant aux distributions prescrites de la température ou du flux thermique à la paroi pour les deux écoulement, sont présentés et analysés.